Heliyon 10 (2024) e35536

Contents lists available at ScienceDirect

Heliyon

journal homepage: www.cell.com/heliyon

Research article

Erythromycin-metal complexes: One-step synthesis, molecular docking analysis and antibacterial proficiency against pathogenic strains

Samuel Attah Egu [a,b,*], Lian Ojotule Abah [a], Jumai Zainab Hussaini [a], Alexander David Onoja [a], Irfan Ali [c], Atiya Habib [d], Urooj Qureshi [d], Sunday Okpanachi Idih [a], Emmanuel Edegbo [e], Lawrence Achimugu [f], Aminu Omale [a], Ojochide Charity Michael [a], Mohammed Umar Adaji [a,b], Jamila Audu Omale [b,g]

[a] Department of Pure and Industrial Chemistry, Kogi State University, Anyigba, Kogi State, Nigeria
[b] Genomics and Molecular Biology Training and Research Laboratory, Kogi State University, Anyigba, Kogi State, Nigeria
[c] H. E. J. Research Institute of Chemistry, International Center for Chemical and Biological Sciences, University of Karachi, Karachi, 75270, Pakistan
[d] Dr. Panjwani Center for Molecular Medicine and Drug Research, International Center for Chemical and Biological Sciences, University of Karachi, Karachi, 75270, Pakistan
[e] Department of Microbiology, Kogi State University, Anyigba, Kogi, Nigeria
[f] Department of Science Education, Kogi State University, Anyigba, Kogi, Nigeria
[g] Department of Biochemistry, Kogi State University, Anyigba, Kogi, Nigeria

ARTICLE INFO

Keywords:
Antibacterial
Culture media
Erythromycin
Metal complexes
Molecular docking
Inocula

ABSTRACT

The study focused on the extraction of free erythromycin from commercially manufactured tablets and the use of metal salts to synthesize erythromycin-metal complexes, specifically involving silver (Ag), nickel (Ni), cobalt (Co), and copper (Cu). The synthesis was confirmed through various methods, including elemental analysis, thermogravimetric analysis, Fourier-transform infrared (FTIR), and UV–visible spectroscopy. The microbiological investigation involved *Salmonella typhi, Escherichia coli, Staphylococcus aureus, Bacillus cereus, Candida albicans,* and *Microsporum canis* as test organisms. The NCCLS broth microdilution reference method was used to determine the minimum fungicidal concentration and minimum inhibitory concentration of the complexes. The synthesized complexes were highly effective against a variety of fungi and bacteria, with compound Ery-Cu having MIC as low as 1.56 mg/mL, Ery-Cu and Ery-Ni with MBCs of 6.25 mg/mL and Ery-Cu having MFC of 6.25 mg/mL. Dose-dependent inhibitory effects were found upon examination of the antimicrobial susceptibility of specific complexes (Cu, Ni, Co and Ag) at varying concentrations of 100, 50, 25 and 12.5 mm/mL. Antibiotic susceptibility testing revealed efficacy against the tested pathogens. The study suggests that the synthesis of erythromycin-metal complexes, coupled with their antibacterial effectiveness against a diverse spectrum of bacteria and fungi, as they showed promising inhibitory properties when tested against a range of test species (*Bacillus cereus*, *Staphylococcus aureus, Escherichia coli, Salmonella typhi, Candida albicans,* and *Microsporum canis*), could lead to the development of innovative antibacterial agents. Molecular docking simulations were used to examine the interactions

* Corresponding author. Department of Pure and Industrial Chemistry, Kogi State University, Anyigba, Kogi State, Nigeria.
E-mail address: samuel.ae@ksu.edu.ng (S.A. Egu).

https://doi.org/10.1016/j.heliyon.2024.e35536
Received 26 February 2024; Received in revised form 25 July 2024; Accepted 30 July 2024
Available online 3 August 2024

between metal complexes with proteins filamentous temperature-sensitive protein Z and lanosterol 14α-demethylase. The study highlights the need for further exploration in pharmaceutical research.

1. Introduction

Metal complexes constitute a fascinating and indispensable class of chemical compounds with profound implications across various scientific disciplines, encompassing biology, chemistry, and materials science [1]. As expounded by Sodhi and Paul, metal complexes are formed through the interaction of metal ions or atoms with neighboring molecules, ions, or ligands via coordinate covalent interactions. Owing to their multifaceted attributes, metal complexes bear immense significance in both practical applications and scholarly pursuits [2]. In recent years, a considerable number of metal complexes of Schiff bases [3–5]have arisen in a variety of areas, including medicinal [6], analytical [7], industrial [8], and antimicrobial applications [9]. Because of their structural composition, these compounds are highly effective against malaria, viral, diabetic, fungal, inflammatory, corrosion, cancer, HIV, antipyretic symptoms, and helminthic infections [10–13]. Erythromycin, an antibiotic that can be taken orally, was first identified in 1952 by McGuire and colleagues. It is derived from a strain of *Streptomyces erythreus*, which was isolated from a soil sample obtained in the Philippine archipelago, as documented in various pharmaceutical and scientific references [14–17]. The medication erythromycin is used to treat respiratory tract infections such as pneumonia, bronchitis, whooping cough, and Legionnaires' disease [17]. It is also employed in the treatment of ear, intestinal, gynecological, urinary tract, and skin infections [18]. Additionally, erythromycin is used to prevent recurrent bouts of rheumatic fever [19].

This threat to life may lead to frequent usage of antibiotics. Because of the frightening rate of upsurge of bacterial infections, as well as the frequent use of antibiotics, drug resistance possesses a global health concern [20]. It is therefore imperative that novel antibacterial compounds be developed to combat this challenge. Although earlier studies provide insightful information about the synthesis and characterization of metal complexes with potential biological uses, the current study has advantages due to its direct investigation of antibacterial activity, applicability, focused assessment of protein interactions, and comparative evaluation of complex efficacy against a wider range of pathogens [21,22]. Ligands containing oxygen, nitrogen, or sulfur atoms have been found to form metal complexes with metals such as copper, zinc, cobalt, and iron. These complexes exhibit improved properties in terms of treating conditions like hypertension, malaria, and microbial infections [23–27]. Transition metal ion complexes have demonstrated their effectiveness as electron transfer agents in various biological processes. Furthermore, they play a significant role in facilitating oxygen transport reactions [28].

A viable strategy toward the development of a more potent bioactive molecule involves the complexation of known drugs with metal ions [29]. The resultant hybrid compound holds the potential to serve as a safer and more efficacious pharmaceutical agent, owing to its synergistic modes of action, improved stability, precision drug delivery, and heightened antibacterial activity. Further research and development in this area could yield inventive treatments addressing antibiotic resistance and enhancing patient outcomes. In 2012, the World Health Organization (WHO) released a report [30] that sparked significant interest among researchers in natural antibiotics. However, it is essential not to disregard the pursuit of synthetically prepared drugs. While natural antibiotics reduce the risk of bacterial resistance [31,32], it's worth noting that structural alterations to existing antibiotics can achieve similar effectiveness.

The choice of erythromycin for this research is justified by its well-established antibacterial properties, extensive clinical use, and availability for research purposes [33]. Cobalt (II) complexes had been reported to be stable and conductive due to the favorable coordination environment of amide-based macrocyclic ligands [34]. This provides a strong basis for the synthesis of erythromycin-Ag, erythromycin-Co, erythromycin-Cu, and erythromycin-Ni complexes. Coordination compounds containing transition metals such as Ru and Co with macrocyclic ligands have been shown to possess antifungal, antibacterial, and anticancer activities [35,36]. Leveraging on this idea implies that the therapeutic efficacy of erythromycin – also a macrocyclic ligand - might be increased by combining it with metals, especially for antibacterial and possibly anticancer uses.

These complexes [34–36] contain metal ions that can interact with nucleic acids and proteins to change their biological structures and functions. This feature is essential for the therapeutic use of erythromycin-metal complexes since it makes tailored medication development possible. For example, cobalt complexes have the ability to selectively target cancer cells via bio-reductive activation; this suggests that erythromycin-Co complexes may be able to take advantage of this mechanism for increased activity. In a similar vein, specific interactions with bacterial cells may be utilized by erythromycin-Ag, erythromycin-Cu, and erythromycin-Ni complexes to enhance antibiotic activity. Therefore, the characteristics and possible uses of transition metal coordination compounds with macrocyclic ligands lend strong support to the formation of these erythromycin-metal complexes. Erythromycin, a widely studied macrolide antibiotic, exhibits broad-spectrum activity against various bacterial pathogens, making it a valuable representative of its antibiotic class for comparative analyses [37]. Factors like accessibility, stability, and solubility influence the selection of specific erythromycin derivatives or formulations for experimental studies, highlighting the importance of these characteristics in research endeavors [38–40]. Researchers may opt for particular erythromycin formulations based on these factors to ensure the practicality and effectiveness of their investigations. Hence, this current research focuses on investigating the antibacterial properties of metal complexes of erythromycin with silver, copper, cobalt and nickel, comparing them with the unaltered parent medication to assess the influence of diverse element complexation on the antibiotic's antibacterial efficacy.

2. Experimental

Analytical research-grade solvents and other metal salts were bought from Sigma-Aldrich and used just as they were received. Pharmaceutically manufactured Erythromycin was obtained from the pharmacy at Prince Abubakar Audu University Teaching Hospital in Anyigba, Nigeria.

2.1. Extraction of erythromycin

Pharmaceutically manufactured Erythromycin (500 mg) was purchased and ground into a fine powder. The powdered particles placed in a beaker were then soaked in 50 mL of methanol for 24 h. The mixture was filtered as the active ingredient was extracted, and the excipient was suspended on the filter. The filtrate was concentrated to obtain free erythromycin.

2.2. General procedure for the synthesis of erythromycin-metal complexes

In an oven-dried round-bottom flask, a mixture of erythromycin (1 mmol) and metal salt (0.5 mmol) in 10 mL of ethanol was stirred at room temperature for 30 min. After the completion of the reaction, the precipitates were filtered and washed with cold water and ethanol to obtain a pure complex. The overall reaction was monitored by thin-layer chromatography (TLC).

2.3. Preparation of culture media

Saboraud Dextrose Agar (SDA) and Nutrient Agar (NA) were used for the microbiological analysis of erythromycin metal complexes (Ag, Ni, Co and Cu) on the pure culture of the tested dermatophytes. The media was prepared and sterilized according to the manufacturer's instructions at ambient laboratory temperature.

2.4. Collection of the test organism

Laboratory isolates of the test organisms (*Salmonella typhi, Escherichia coli, Staphylococcus aureus, Bacillus cereus, Candida albicans and Microsporum canis*) were obtained from the stock culture in the laboratory department of Microbiology at Kogi State University, Anyigba.

2.5. Preparation of fungal inoculum

Stock inoculum suspensions of fungal isolates were prepared from a 7-15-day-old culture grown on SDA at ambient temperature ($28 \pm 2\ ^{\circ}C$). Matured colonies were covered with 10 mL of sterile saline (0.85 %) and a drop of polysorbate (tween 80 sigma). The surfaces were scraped using the tip of a pasture pipette. The resulting mixture of conidial and hyphal fragments was withdrawn and transferred to sterile test tubes. Heavy particles were allowed to settle for 15 min at room temperature ($28 \pm 2\ ^{\circ}C$). The upper suspension was mixed using a vortex mixer for 15 s. The turbidity of the supernatants was measured using a spectrophotometer at a wavelength of 530 nm and transmission was adjusted to 65–70 %. Each suspension was diluted 1:50 in SDA to obtain conidia suspension of 0.5 McFarland (approximately 10 SFU/mL) standards, respectively. Plate counts were performed to verify the conidial concentration by plating 0.01 mL of the adjusted conidial suspension to determine the viable number of conidia and millimeters [41].

2.6. Preparation of bacterial inoculum

Using physiological saline, bacterial cell suspensions were prepared from 24 cultures grown on nutrient agar. The turbidity of the supernatants was measured using a spectrophotometer at a wavelength of 530 nm and transmission was adjusted to 65–70 %. Each suspension was diluted 1:50 in NA to obtain colony-forming units of 0.5 McFarland (approximately 10 CFU/mL) standards, respectively. Plate counts were performed to verify the colonial concentration by plating 0.01 mL of the adjusted conidial suspension to determine the viable number of colonies and millimeters [41].

2.7. Preliminary antimicrobial screening of erythromycin metal complexes (Ag, Ni, Co and Cu)

The preliminary antimicrobial screening for erythromycin metal complexes (Ag, Ni, Co and Cu) was carried out using the agar incorporation method as described by Refs. [28,29]. 0.5 g/mL of the erythromycin metal complexes were mixed with 15 mL of nutrient agar (for bacterial isolates) and Sabouraud dextrose agar (for fungal isolates) after cooling and solidification of the medium. The seeding was carried out by inoculating the test organisms on the plates. A control plate that contains the organism and the medium alone was also set up. The treated and control Petri dishes were incubated at ambient laboratory conditions until growth was apparent on the control plates. The presence of growth (+) is a negative test (indicating the non-potency of the test material) and the absence of growth (−) is a positive test (indicating the potency of the test material).

2.8. Determination of the antimicrobial activity of erythromycin metal complexes

2.8.1. Preparation of metal solutions

The stock solutions of all the metal complexes (Ag, Ni, Co and Cu) were prepared in water at varying concentrations. The complexes were ten-fold serially diluted as described by the National Committee for Clinical Laboratory Standards 41, followed by a further two-fold dilution in broth to yield the final concentrations required for testing.

2.8.2. Antimicrobial susceptibility testing of the complexes

Using physiological saline, cell suspension was prepared to give concentrations equivalent to 0.5 McFaland (106). 0.01 mL of organisms was used for further inoculation and further testing. Hundred microliters (100 μL) of the standardized colony suspension (106) were evenly spread on NA media. Wells were then bored into the agar media using a sterile 6 mm cork borer and then carefully filled with the extracts. The plates were allowed to stand on the laboratory bench for 1 h to allow for proper diffusion of the erythromycin and metal complexes into the media. Hexane was used as a negative control, while ketoconazole and erythromycin (25 mg/mL) were used as positive controls for fungi and bacteria, respectively. The plates were incubated and later examined for zones of inhibition [42].

2.9. Determination of minimum inhibitory concentration (MIC) and minimum fungicidal concentration (MFC) of the complexes

The NCCLS broth microdilution reference method was performed according to the NCCLS M27-P [43] with slight modifications. A total of 11 test tubes (Khan tubes) were used for the determination of MIC. 1 mL of broth was dispensed into test tubes 2–11 each. From the stock solution of the metal complex (100 mg/mL), 1 mL was dispensed into tube 1 and another mL into tube 2. From the content in tube 2, two-fold serial dilutions were carried out up to tube 9. From tube 9, 1 mL was pipetted out and discarded. The concentrations in the tubes were 100, 50, 25, 12.5, 6.25, 3.125, 1.563, 0.78, and 0.39 mg/mL. A total of 100 aliquots of each organism previously diluted to give 0.5 spores/colony/mL were dispensed into tubes 1 to 11, except for tube 10. To tube 10, 1 mL of sterile broth was added. Tube 1, which contained 1 mL of the metal complex and 1 mL of the spore solution of the test organism, served as the control for the metal complex; tube 10, which contained 1 mL of sterile SDB, served as the control for the sterility of the medium; and tube 11, which contained 1 mL of the solution of the test organism and 1 mL of sterile SDB, served as the control for the viability of the test organism. All tubes were incubated at ambient temperature until growth was apparent in the growth control tubes. Tubes were observed visually

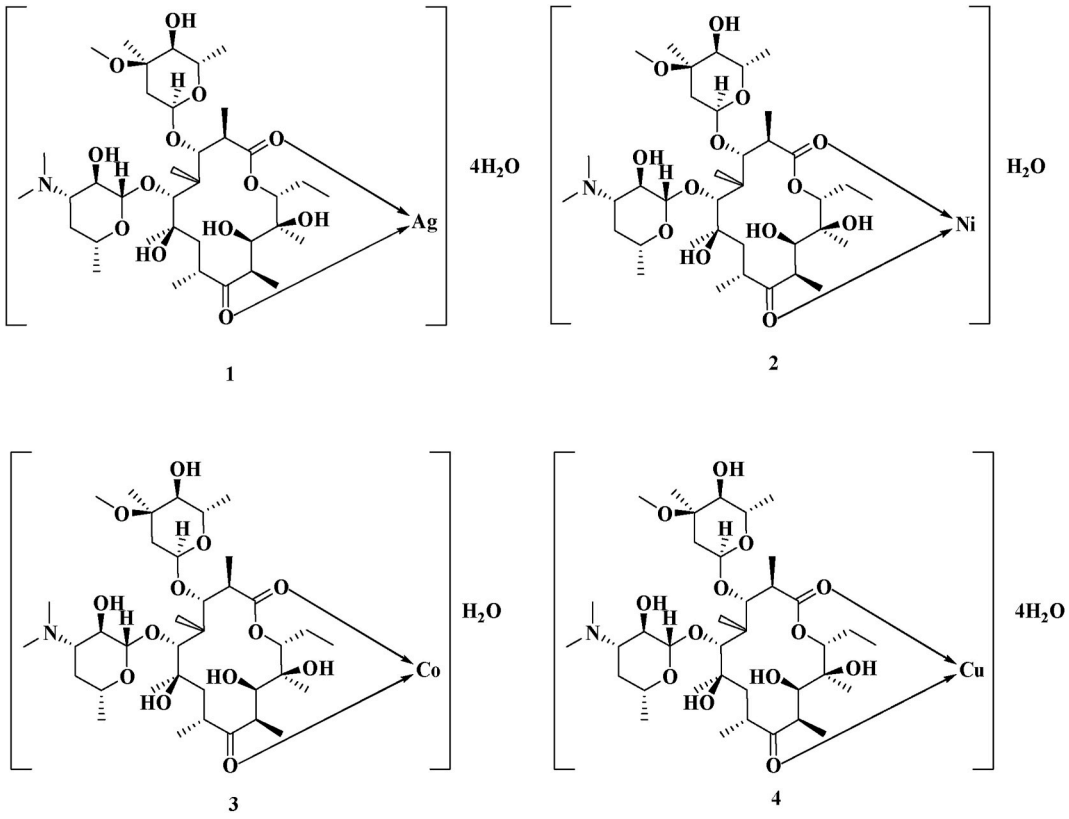

Fig. 1. Proposed structure of the erythromycin-based complexes.

for growth based on turbidity or cloudiness. The lowest concentration of metal complex that produced complete inhibition was regarded as the MIC. After the MIC determination, 100 aliquots of broth were transferred from all tubes showing no growth and from the first tube in which growth was detectable to plates of solid medium. The plates were incubated at ambient laboratory conditions for 72 h. The complex with the complex with the lowest concentration, for which subculture did not show any growth, was regarded as the MFC.

2.10. Molecular docking simulation

Molecular docking simulation were carried out using Molecular Operation Environment (MOEv2019.01) [44]. The crystallographic structure having PDB ID: 3VOB and 5JLC was retrieved from Protein Data Bank (PDB) having the resolution of 2.70 and 2.40 Å from x-ray crystallography respectively (https://www.rcsb.org/) [45,46]. The 3D structures were prepared using structure preparation module in MOEv2019.01 via geometry optimization and energy minimization using Amber10:EHT force field. All target compounds were sketched using Chemdraw 15.0, were also prepared using standard protocol of MOEv2019.01 using MMFF94x force field for energy minimization and energy gradient convergence criteria of 0.1 kcal/mol. The validation process was performed by re-docking the original ligands into the active site of receptors. In total 30 conformations of ligand were generated. The highest scored conformation of ligand complex was selected for further reconnaissance of binding pattern using Protein-Ligand Interaction Profiler (PLIP) while interaction diagram were produced using UCSF Chimera 1.16 software [47].

2.11. ADMET profiling

Swiss ADME is an open-source platform to predict ADME (Adsorption, Distribution, Metabolism, and Excretion) properties of compounds [48]. Highest scoring compounds were subjected for ADME profiling of the compounds. The evaluation of Physicochemical properties such as lipophilicity, water solubility alongside pharmacokinetics, drug-likeness and medicinal chemistry aspects of the compounds were considered. Furthermore, in silico toxicity assessments were conducted the highest scoring compounds using ProTox-II webserver [49].

3. Results and discussion

3.1. Chemistry

The erythromycin-based complexes (1–4) (Fig. 1) were synthesized in a one-step reaction procedure that involved the reaction of erythromycin and the metal salts within 30 min (Scheme-1). The formation of the target compounds (1–4) was confirmed by spectroscopic data obtained from FTIR, ultimate analysis, TGA, and UV–Vis spectroscopes. The formation of the complexes was confirmed by their behavior under varying temperature conditions, a shift in the maximum wavelength, and a shift in the FTIR vibrations.

3.2. Detailed spectral study of the complexes

3.2.1. UV–visible analysis

The UV–visible spectra of the ligand and its metal complexes were recorded in ethanol. The electronic transitions in the ligands and the ligand-metal charge transfer transitions are evident from the lambda maximum value observed from their UV–visible spectra: Ery-Ag 1 (λ_{max}: 320 nm), Ery-Ni 2 (λ_{max}: 200 nm), Ery-Co 3 (λ_{max}: 280 nm), and Ery-Cu 4 (λ_{max}: 280 nm). Free erythromycin had been reported to have a λ_{max} of 285 nm [50].

3.2.2. FTIR analysis

The surface chemistry of the erythromycin complexes was studied using FTIR spectroscopy to confirm the coordination between the metals and the ligand used. The FTIR spectra of the complexes display distinct bands associated with the ligand's characteristics

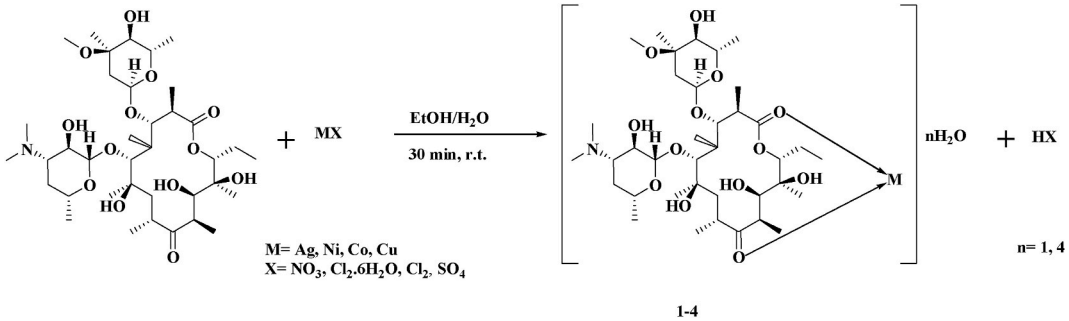

Scheme 1. Reaction scheme for synthesis of erythromycin-based complexes.

Table 1
FTIR results of erythromycin and the complexes.

Compound	-OH (cm^{-1})	-C-H (cm^{-1})	-C=O (cm^{-1})	-C-O-C
Erythromycin	3302	2922	1722	1163
Ery-Ag complex	3384	2915	1512	1111
Ery-Ni complex	3310	2915	1551	1111
Ery-Co complex	3355	2915	1521	1103
Ery-Cu complex	3392	2915	1580	1111

(Table 1). Specifically, bands falling within the 1409–1461 to 1461 cm^{-1} range signify vibrations related to C–N bonds. In the 1103 to 1163 cm^{-1} region, the observed bands can be attributed to the stretching mode of C–O–C bonds, while those spanning from 3302 to 3922 cm^{-1} are assigned to O–H stretching vibrations. Bands in the 1513-1722 cm^{-1} range correspond to –C=O functionalities. Furthermore, the bands at 2915 and 2922 cm^{-1} are indicative of C–H stretching, with the former being associated with the complexes and the latter with the ligand. The FTIR spectra provide compelling evidence that the formation of metal complexes likely resulted from the interaction of lone pairs on the oxygen atom of the carbonyl groups in the ligand, as evident from the noticeable variation in the –C=O peaks (indicated by the arrow in Fig. 2).

3.3. Ultimate analysis (elemental analysis)

The elemental analysis results for the four erythromycin complexes are shown in Table-2. Following the determination of the experimental percentages of carbon (C), hydrogen (H), nitrogen (N), and oxygen (O), the percentages based on the chemical formula of erythromycin complexes were compared to the results. For every complex, the data demonstrate a close match between the calculated and experimental values, indicating the precision and structural integrity of the synthesis process.

3.4. Thermogravimetric analysis

The complexes were subjected to thermogravimetric and differential thermal (TG/DT) analysis under an air atmosphere with a heating rate of 10 °C per minute, covering a temperature range from room temperature to 700 °C. In Table-3, a comparison of the erythromycin-based complexes showed different thermal properties and patterns of breakdown. All four complexes showed a common beginning phase in the first stage (Stage I) that was characterized by the release of water molecules (dehydration). For the Copper (Cu) complex, this stage was found between 23 and 28 °C, for the Silver (Ag) complex between 28 and 285 °C, for the Cobalt (Co) complex between 28 and 250 °C, and for the Nickel (Ni) complex between 28 and 340 °C. The resultant mass losses, which ranged from 2.23 % to 8.3 %, closely matched the computed values (Fig. 3). Differential Thermal Analysis (DTA) was used to determine the maximum rate of mass loss, as shown in Table-3. During the second phase, there was a mass loss of 86.0 % (or 79.0 %) for the silver (Ag) complex between 285 °C and 440 °C. On the other hand, the cobalt (Co) complex showed its second stage at 250 °C–390 °C, losing 47.5 % of its mass (estimated at 42.0 %). The second stage was displayed by the copper (Cu) complex between 260 °C and 390 °C, with a mass loss of 26.0 % (estimated as 29.0 %), and by the nickel (Ni) complex between 240 °C and 400 °C, with a mass loss of 47.4 % (estimated as 43.0 %). All of the complex's mass losses during the second stage were very similar to the numbers that were calculated. The silver (Ag) complex demonstrated this phase at temperatures higher than 440 °C in the third stage, resulting in a mass loss of 13.4 %, which was in line with the calculated value of 13.0 %. Comparably, the third stage of the cobalt (Co) complex took place between 390 and 440 °C, resulting in a mass loss of 50.3 % (or 45.0 %) of the original material. Between 390 °C and 560 °C, the Copper (Cu) complex showed its Stage III, with a mass loss of 64.0 % (estimated as 58.0 %), and between 400 °C and 510 °C, the Nickel (Ni) complex showed its Stage III, with a mass loss of 50.2 % (estimated as 54.0 %). At the stage of complete decomposition (Stage IV or V), the ligand undergoes complete decomposition, ultimately yielding metal oxide as the ultimate residual product. That of Ery-Ag was observed at temperatures above 440 °C, Ery-Co above 630 °C, Ery-Cu above 590 °C, and Ery-Ni above 510 °C. Mass losses of 13 % (calculated 13 %), 9.2 %

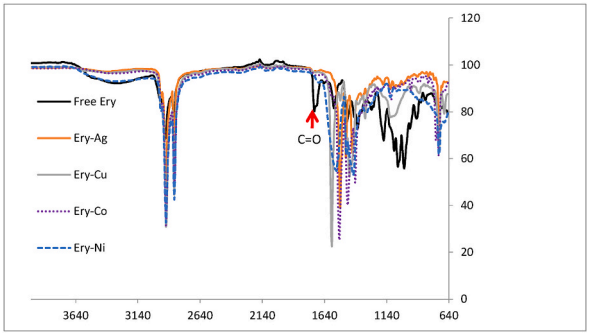

Fig. 2. FTIR spectra of free erythromycin and erythromycin-based metal complexes.

Table 2
Result of elemental analysis of the complex.

Complex	C (%) found (calcd)	H (%) found (calcd)	N (%) found (calcd)	O (%) found (calcd)
Ery-Ag	43.42 ± 0.3 (48.68)	9.80 ± 0.3 (8.17)	0.35 ± 0.1 (1.53)	27.59 ± 0.2 (29.80)
Ery-Co	42 34 ± 0.21 (55.03)	7.21 ± 0.43 (8.24)	1.23 ± 0.56 (1.73)	28.32 ± 0.54 (27.74)
Ery-Cu	45.72 ± 0.12 (51.17)	8.40 ± 0.34 (8.59)	0.75 ± 0.6 (1.61)	30.39 ± 0.6 (31.32)
Ery-Ni	42.73 ± 0.52 (54.89)	8.76 ± 0.45 (8.47)	0.45 ± 0.3 (1.73)	29.34 ± 0.54 (27.67)

Table 3
Thermogravimetric analysis of the metal complexes.

Complex	Temp. (°C)	DTA (°C)	Stage	Mass loss (g) Found (Calcd. %)	Assignment
$C_{37}H_{74}AgNO_{17}$	28–285	270	I	8.0 (8.0)	Dehydration of H_2O
	285–440	440	II	86.0 (79.0)	$C_{37}H_{66}NO_{12}$
	>440	750	III	13.4 (13)	AgO
$C_{37}H_{74}CoNO_{17}$	28–250	180	I	2.23 (3.0)	Dehydration of H_2O
	250–390	300	II	47.5 (42.0)	$C_{21}H_{36}O_6$
	390–440	440	III	50.3 (45)	$C_{16}H_{30}NO_7Co$
	440–630	625	IV	5.7 (5.0)	C_2H_6N
	>630	630	V	9.2 (10.0)	CoO
$C_{37}H_{74}CuNO_{17}$	23–260	230	I	8.3 (8.0)	Dehydration of H_2O
	260–390	330	II	26.0 (29.0)	$C_8H_{15}CuNO_3$
	390–560	420	III	64.0 (58.0)	$C_{29}H_{51}O_{10}$
	>560	690	IV	9.0 (6.0)	CuO
$C_{37}H_{68}NiNO_{14}$	28–340	240	I	2.23 (2.0)	Dehydration of H_2O
	240–400	330	II	47.4 (43.0)	$C_{21}H_{36}O_6$
	400–510	480	III	50.2 (54.0)	$C_{16}H_{30}NNiO_7$
	>510	720	IV	9.0 (11.0)	NiO

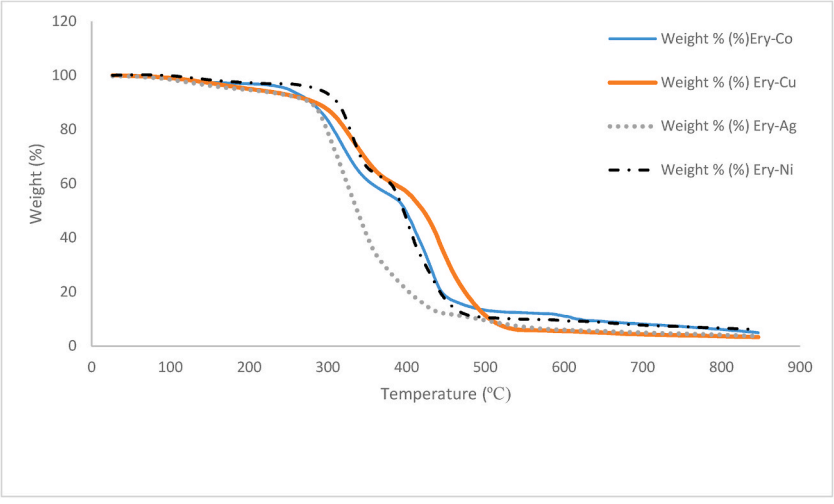

Fig. 3. TG curve of Ery-Ag, Ery-Ni, Ery-Co and Ery-Cu. Heating rate: 10 °C/min.

(calculated 10 %), 9 % (calculated 6 %), and 9 % (calculated 11 %) were observed for Stages IV and V for Ery-Ag, Ery-Co, Ery-Cu, and Ery-Ni, respectively (Fig. 4).

Table-4 revealed the results of the preliminary antimicrobial activity of erythromycin metal complexes (Ag, Ni, Cu and Co) and pure erythromycin against the test organisms. All the metal complexes had activity against the tested organisms. Pure erythromycin exhibited antibacterial activity against the bacterial isolates, while ketoconazole had antifungal activity against the fungal isolates tested.

At a concentration of 100 mg/mL, *Bacillus cereus* had an inhibition zone of 19 mm, *Staphylococcus aureus, Escherichia coli* and *Salmonella typhi* had inhibition zones of 17 mm, *Candida albicans* had an inhibition zone of 13 mm and *Microsporum canis* had an inhibition zone of 14 mm. At a concentration of 50 mg/mL, *Bacillus cereus* had an inhibition zone of 16 mm; *Staphylococcus aureus* and *Salmonella typhi* had 15 mm; *Escherichia coli* had14 mm; *Candida albicans* and *Microsprum canis* had 11 mm. At a concentration of 25

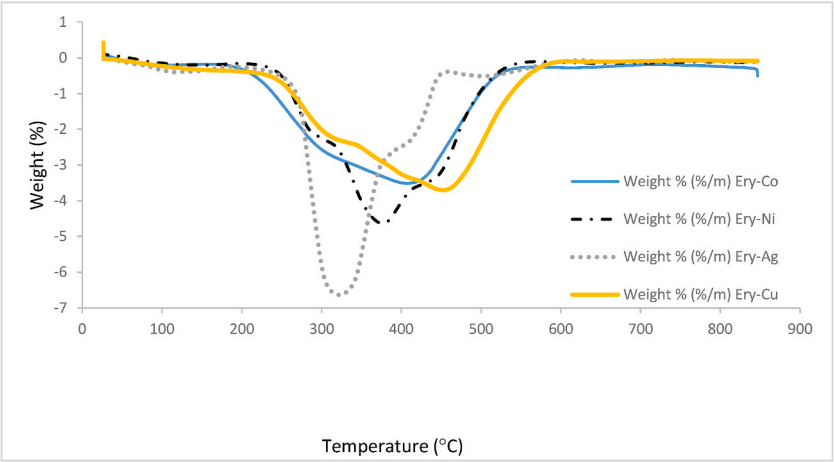

Fig. 4. DTA curve of Ery-Ag, Ery-Ni, Ery-Coand Ery-Cu. Heating rate: 10 °C/min.

Table 4
Preliminary antimicrobial susceptibility of erythromycin metal complexes (Cu, Ni, Co and Ag) against the test organisms.

Organisms	Erythromycin Complexes				Ery	Ket
	Ery-Cu	Ery-Ni	Ery-Co	Ery-Ag		
Bacillus cereus	–	–	–	–	–	+
Staphylococcus aureus	–	–	–	–	–	+
Escherichia coli	–	–	–	–	–	+
Salmonella typhi	–	–	–	–	–	+
Candida albicans	–	–	–	–	+	–
Microsporum cania	–	–	–	–	+	–

Key: Ket – ketoconazole, 25 mg/mL for fungi, Ery – Erythromycin, 25 mg/mL for bacteria. (–) – absence of microorganism, (+) – presence of microorganism.

mg/mL, *Bacillus cerues* had inhibition zones of 14 mm, *Staphylococcus aureus* and *Salmonella typhi*, 13 mm, *Escherichia coli*, 12 mm, *Candida albicans*, 8 mm, and *Microsporum canis*, 10 mm. At a concentration of 12.5 mg/mL, *Bacillus cereus* had an inhibition zone of 12 mm. *Staphylococcus aureus* and *Salmonella typhi* had 11 mm, *Eschrichia coli* had 10 mm, *Candida albicans* had 6 mm, and *Microsporum canis* had inhibition zones of 8 mm (Table-5).

Table-6 shows the antimicrobial susceptibility of the Erthromycin/Nickel complex at different concentrations of 100 mg/mL, 50 mg/mL, 25 mg/mL, and 12.5 mg/mL mg/mL, *Bacillus cereus* and *Salmonella typhi* had inhibition zones of 18 mm, *Staphylococcus aureus* and *Escherichia coli* had inhibition zones of 16 mm, *Candida albicans* had 15 mm and *Microsporum canis* had 14 mm. 50 mg/mL, *Bacillus cereus* had an inhibition zone of 15 mm, *Staphylococcus aureus* and *Escherichia coli* had an inhibition zone of 14 mm, *Salmonella typhi* had 16 mm, *Candida albicans* had 13 mm and *Microsporum canis* had 12 mm. At the concentration of 25 mg/mL, *Bacillus cereus* had inhibition zone of 13 mm, *Staphylococcus aureus* and *Escherichia coli* had inhibition zone of 12 mm, *Salmonella typhi* 14 mm, *Candida albicans* had 11 mm and *Microsporum canis* had 9 mm. At *Bacillus cereus* had an inhibition zone of 13 mm at 25 mg/mL, *Staphylococcus aureus* and *Escherichia coli* had 12 mm, *Salmonella typhi* had 14 mm, *Candida albicans* had 11 mm, and *Microsporum canis* had 9 mm. concentration of 12.5 mg/mL, *Bacillus cereus* had an inhibition zone of 11 mm, *Staphylococcus aureus* and *Escherichia coli* had an inhibition zone of 10 mm, *Salmonella typhi* had a zone of 12 mm, *Candida albicans* had an inhibition zone of 8 mm and *Microsporum canis* also had an inhibition zone of 8 mm.

Table 5
Antimicrobial Susceptibility of Ery-Cu complex at different concentrations of 100 mg/mL, 50 mg/mL, 25 mg/mL and 12.5 mg/mL.

Organism	Complex Concentration (mg/mL)				Positive Control	Negative Control
	100	50	25	12.5		
Bacillus cereus	19	16	14	12	11	0
Staphylococcus aureus	17	15	13	11	10	0
Escherichia coli	17	14	12	10	11	0
Salmonella typhi	17	15	13	11	11	0
Candida albicans	I3	11	8	6	10	0
Microsporum canis	14	11	10	8	11	0

Key: Ket-ketoconazole, 25 mg/mL for fungi, Ery-Erythromycin, 25 mg/mL for bacteria. Negative control - Hexane.

Table 6
Antimicrobial Susceptibility of Ery-Ni complex at different concentrations.

Organism	Complex Concentration (mg/mL)				Positive Control	Negative Control
	100	50	25	12.5		
Bacillus cereus	18	15	13	11	11	0
Staphylococcus aureus	16	14	12	10	10	0
Escherichia coli	16	14	12	10	11	0
Salmoneella typhi	18	16	14	12	12	0
Candida albicans	15	13	11	8	10	0
Microsporum Canis	14	12	9	8	11	0

Key: Ket – ketoconazole, 25 mg/mL for fungi, Ery – Erythromycin, 25 mg/mL for bacteria. Negative control - Hexane.

Table-7 revealed the antimicrobial susceptibility of the Erthromycin/Nickel complex at different concentrations of 100 mg/mL, 50 mg/mL, 25 mg/mL, and 12.5 mg/mL. At concentrations of 100 mg/mL, *Bacillus cereus* and *Salmonella typhi* had zones of inhibition of 20 mm, *Staphylococcus aureus* had 21 mm, *Escherichia coli* had 19 mm. *Candida albicans* and *Microporum canis* had 16 mm, At a concentration of 50 mg/mL, *Bacillus cereus* had a zone of inhibition of 18 mm, *Staphylococcus aureus* 19 mm, *Salmonella typhi* and *Escherichia coli* 17 mm, *Candida albicans* had 14 mm and *Microsporum canis* had 13 mm. At a concentration of 25 mg/mL, *Bacillus cereus* had a zone of inhibition of 16 mm, *Staphylococcus aureus* 16 mm, *Salmonella typhi* and *Escherichia coli* 15 mm, *Candida albicans* had 12 mm and *Microsporum canis* had 11 mm. At concentrations of 12.5 mg/mL, *Bacillus cereus* and *Escherichia coli* had zones of inhibition of 13 mm, *Staphylococcus aureus* had 14 mm, *Salmonella typhi* had 11 mm, *Candida albicans* had 10 mm and *Microsporum canis* had 9 mm.

Table-8 shows the antimicrobial susceptibility of the erthromycin/silver complex at different concentrations of 100 mg/mL, 50 mg/mL, 25 mg/mL and 12.5 mg/mL. At concentrations of 100 mg/mL, *Bacillus cereus*, *Escherichia coli* and *Salmonella typhi* had inhibition zones of 22 mm, *Staphylococcus aureus* had inhibition zones of 21 mm, *Candida albicans* and *Microsporum canis* had inhibition zones of 17 mm. At concentrations of 50 mg/mL, *Bacillus cereus* and *Escherichia coli* had inhibition zones of 20 mm, *Staphylococcus aureus* and *Salmonella typhi* had 19 mm, *Candida albicans* and *Microsporum canis* had 15 mm. At a concentration of 25 mg/mL, *Bacillus cereus* had an inhibition zone of 18 mm; *Staphylococcus aureus* and *Escherichia coli* had inhibition zones of 17 mm; *Salmonella typhi* had inhibition zones of 16 mm; *Candida albicans* and *Microsporum canis* had inhibition zones of 13 mm. At a concentration of 12.5 mg/mL, *Bacillus cereus* had an inhibition zone of 16 mm; *Staphylococcus aureus* and *Salmonella typhi* had inhibition zones of 14 mm; *Candida albicans* and *Microsporum canis* had inhibition zones of 11 mm.

Table-9 shows the minimum inhibitory concentration (MIC) and minimum cidal (bactericidal, MBC, or fungicidal, MFC) concentrations. The minimum inhibitory concentration (MIC) of erythromycin/cupper complex was 1.56 mg/mL for *Bacillus cereus*, and *Candida albicans*, 3.125 mg/mL for *Staphylococcus aureus*, *Escherichia coli*, *Salmonella typhi* and *Microsporum canis*, and was cidal to all the organisms tested at the concentration of 25 mg/mL. Erythromycin/nickel complex had MICs of 3.125 mg/mL against B. cereus, *Staph. aureus*, *C. albicans*, and *M. canis*; 6.25 mg/mL against *E. coli* and *S. typhi*; and was cidal to *B. cereus* and *C. albicans* at a concentration of 6.25 mg/mL; *Staph. aureus*, E. *coli*, and *M. canis* at 12.5 mg/mL; and *S. typhi* at25 ml/mL erythromycin/cobalt complex mic against *B. cereus* and *Staph. aureus* was 3.125 mg/mL, *E. coli, S. typhi, C. albicans,* and *M. canis* was 6.25 mg/mL, and was cidal to *B. cereus*, *Staph. aureus*, *S. typhi*, and *M. canis* at a concentration of 6.25 mg/mL, and *E. coli* and *C. albicans* at 12.5 mg/mL. The erythromycin/silver complex had MICs of 3.125 mg/mL against *B. cereus*, *Staph. aureus*, and *M. canis* and 6.25 mg/mL against *E. coli, S. typhi* and *C. albicans*. It was cidal to *B. cereus*, *S. aureus*, and *S. typhi* at a concentration of 12.5 mg/mL. *E. coli*, *C. albicans* and *M. canis* at 25 mg/mL.

The antimicrobial activities of the synthesized complexes were compared with those of reference drugs (ketoconazole for fungi and erythromycin for bacteria). This was done by measuring their zone of inhibition diameter (mm). A previous report has shown that Ni^{2+}, Cu^{2+}, and Zn^{2+} complexes possessed moderate antibacterial activities with the free ligand as a result of the chelation [51,52]. This is in agreement with the results reported in the literature, indicating a better performance of complexes over their free ligand [53,54]. Sahraei et al. [55] also reported the antibacterial superiority of the copper (ii) complex of a 4-amino antipyrine derivative over its free ligand. In a recent report by Refs. [56,57], some Cu(II) complexes performed better than their macrocyclic ligands, to the extent of

Table 7
Antimicrobial Susceptibility of Ery-Co complex at different concentrations.

Organism	Complex Concentration (mg/mL)				Positive Control	Negative Control
	100	50	25	12.5		
Bacillus cereus	20	18	16	13	11	0
Staphylococcus aureus	21	19	16	14	10	0
Escherichia coli	19	17	15	13	11	0
Salmoneella typhi	20	17	15	11	12	0
Candida albicans	16	14	12	10	10	0
Microsporum Canis	16	13	11	9	11	0

Key: Ket – ketoconazole, 25 mg/mL for fungi, Ery – Erythromycin, 25 mg/mL for bacteria. Negative control - Hexane.

Table 8
Antimicrobial Susceptibility of Ery-Ag complex at different concentrations.

Organism	Complex Concentration (mg/mL)				Positive Control	Negative Control
	100	50	25	12.5		
Bacillus cereus	22	20	18	16	11	0
Staphylococcus aureus	21	19	17	14	10	0
Escherichia coli	22	20	17	15	11	0
Salmoneella typhi	22	19	16	14	12	0
Candida albicans	17	15	13	10	10	0
Microsporum Canis	17	15	13	11	11	0

Key: Ket-ketoconazole, 25 mg/mL for fungi, Ery-Erythromycin, 25 mg/mL for bacteria. Negative control - Hexane.

Table 9
Minimum inhibitory concentration (MIC) and minimum cidal (bactericidal, MBC/fungicidal, MFC) concentrations.

Dermatophytes	Ery-Cu (mg/mL)		Ery-Ni (mg/mL)		Ery-Co (mg/mL)		Ery-Ag (mg/mL)	
	MIC	MFC	MIC	MFC	MIC	MFC	MIC	MFC
Bacillus cereus	1.56	6.25	3.125	6.25	3.125	12.5	3.125	12.5
Staphylococcus Aureus	3.125	6.25	3.125	12.5	3.125	12.5	3.125	12.5
Escherichia coli	3.125	6.25	6.25	12.5	6.25	25	6.25	25
Salmonella typhi	3.125	6.25	6.25	25	6.25	12.5	6.25	12.5
Candida albicans	1.56	6.25	3.125	6.25	6.25	25	6.25	25
Microsporum Canis	3.125	6.25	3.125	12.5	6.25	12.5	3.125	25

Key: MIC- Minimum inhibitory concentration MFC- Minimum cidal concentration.

having additional applications as antibacterial and antifungal agents. The high water solubility of amide-based Co(II) complexes provided an antimicrobial advantage over their ligand counterparts [58]. Only in rare cases have the ligands shown more activity than their corresponding complexes, although the same report expressed better antifungal activities for the complexes compared to the ligands [59].

Herein, we have incorporated Ag, Ni, Cu, and Co metals into erythromycin and have screened them against bacterial strains as indicated in Tables 4–9 The observation in this report is that the complexes had both antibacterial and antifungal activities, as opposed to the free ligand, which possessed only antibacterial activities. The activities of the complexes can be attributed to the disappearance of the polarity of the metal, leading to the orbitals of ligands overlapping to share the metal's positive charge with the donor groups during chelating [53]. This chelating process favors the lipophilicity of the metal atoms, subsequently inhibiting the metal binding sites of the microbes [60,61].

The entire process increases the antibacterial action of the complexes. This study has revealed that erythromycin's usability can be extended by complexing it with metals, making it potentially "sought after" in the pharmaceutical industry. The activities of the complexes in this present work can compete favorably with previous reports. The zones of inhibition herein lie between 6 mm and 22 mm, comparable with the report of Subhash and co-workers, falling within a similar range [52,62].

3.5. Structure activity relationship

In the process of finding and developing new drugs, it is critical to comprehend the biological properties of synthetic molecules. They can be used to identify safety profiles and possible therapeutic applications by looking at how they affect cellular processes. Through comparative research, we can clarify structure-activity links that are essential for optimizing medication candidates.

In comparison, as shown in Fig. 5, the compound Ery-Cu (MIC = 1.56 mg/mL) showed better activity against *B. cereus*, while the other three compounds are at par (MIC = 3.125 mg/mL). All the complexes showed equal potency against *S. aureus*, while Ery-Cu (MIC = 3.125 mg/mL) showed the highest activity against *E. coli* and *S. typhi*. The other complexes also had similar activities. Against *C. albicans*, Ery-Cu (MIC = 1.56 mg/mL) also had better activity, followed by Ery-Ni (MIC = 3.125 mg/mL), and then Ery-Ag and Ery-Co at MICs of 6.25 mg/mL each. Ery-Cu (MIC = 3.125 mg/mL), Ery-Ni (MIC = 3.125 mg/mL), and Ery-Ag (MIC = 3.125 mg/mL) all had better activities than Ery-Co (MIC = 12.5 mg/mL).

In relation to MBC/MFC (Fig. 6), Ery-Cu and Ery-Ni with MBCs of 6.25 mg/mL showed better activity than Ery-Co and Ery-Ag, each having MBC of 12.5 mg/mL against *B. cereus*. Against *S. aureus*, Ery-Cu (MBC = 6.25 mg/mL) showed better activity than the remaining compounds, which had an MBC of 12.5 mg/mL. Against *E. coli*, Ery-Cu (MBC = 6.25 mg/mL) displayed the best activity, followed by Ery-Ni (MBC = 12.5 mg/mL), and then Ery-Co and Ery-Ag had the same activity (MBC = 25 mg/mL). When tested against *S. typhi*, Ery-Cu still displayed the highest activity (MBC = 6.25 mg/mL), followed by Ery-Co (MBC = 12.5 mg/mL), Ery-Ag (MBC = 12.5 mg/mL), and then Ery-Ni (MBC = 25 mg/mL). Ery-Cu (MFC = 6.25 mg/mL) and Ery-Ni (MFC = 6.25 mg/mL) showed better activity than Ery-Co (MFC = 25 mg/mL) and Ery-Ag (MFC = 25 mg/mL) against *C. albicans*. Ery-Cu (MFC = 6.25 mg/mL) surpassed Ery-Ni (MFC = 12.5

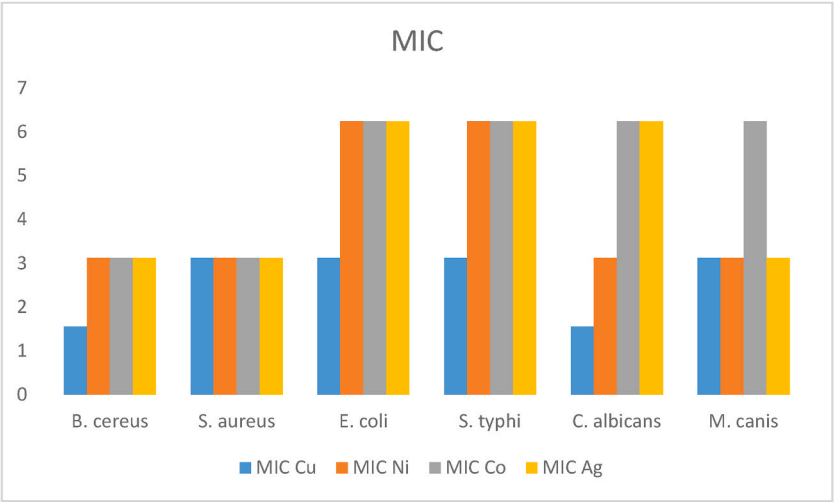

Fig. 5. MIC of studied complexes.

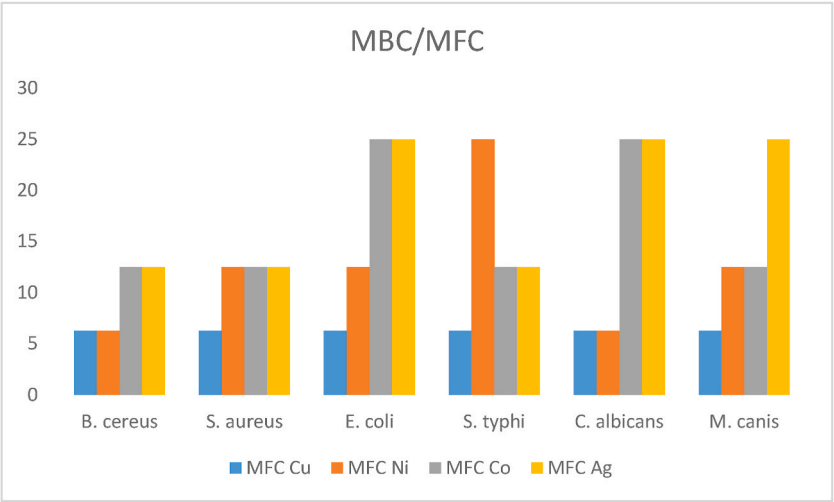

Fig. 6. MFC of studied complexes.

mg/mL) and Ery-Co (MFC = 12.5 mg/mL), and then finally Ery-Ag (MFC = 25 mg/mL) against *M. canis*. Generally, Ery-Cu showed more potency in comparison with other studied complexes.

3.6. Molecular docking simulation

In current study, molecular docking simulation is used to unravel the potential connections and binding strength in order to anticipate the best binding orientation and affinity between the protein and ligand. In this study, the proteins pdb 3VOB and 5JLC were selected due to their critical roles in bacterial cell function. Consequently, molecular docking studies were conducted to explore potential interactions between the active site of 3VOB: FtsZ (filamentous temperature-sensitive protein Z), a bacterial protein involved in cell division, and lanosterol 14α-demethylase (CYP51), an essential enzyme in the ergosterol biosynthetic pathway of fungi. These interactions were analyzed against synthesized metal complexes to aid in the structure-based design of new drugs [63–65].

At first, Redocking experiment was first performed using different algorithm, out of which Alpha triangle with Alpha HB and ASE as scoring function for 3VOB and Alpha Triangle with Affinity dG with GBIV/WSA dG a s scoring function for 5JLC using induced fit protocol were selected based on Root Mean Square Deviation (RMSD) found to be less than 3 Å i.e., 0.69 Å for 3VOB and 1.84 Å for 5JLC in Fig. 7a and b. According to the docking results metal complexes of nickel and copper displayed the best results as compared to other complexes and standards.

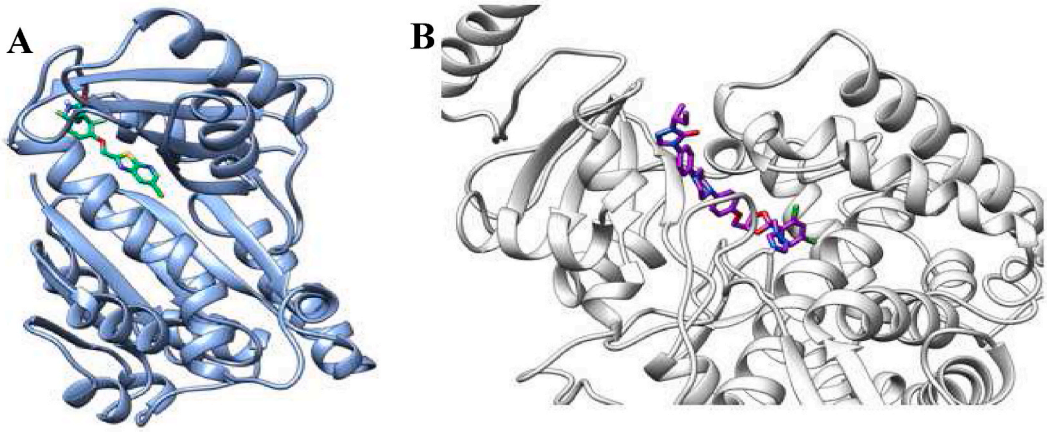

Fig. 7. Re-docked pose of 3VOB (a) and 5JLC (b) with its cognate ligand having lowest RMSD.

3.6.1. *Inter-molecular interaction pattern of 3VOB*

The nickel complex displayed the hydrophobic interactions with Leu200 and Asn263 and a total of three electrostatic interactions were found to be generated moderately weak interactions with Gly196, Gly227 and a strong interaction with Val310 at a distance of 3.5, 3.0 and 2.5 Å respectively with binding affinity of −41.70 kcal/mol. However, the copper complex was observed to maintain hydrophobic interactions with Asp199, Ile228 and Val297. It established three weak electrostatic interactions with Ile197, Asn263 and Val310 having distances of 3.2, 3.2 and 3.4 Å with the biding affinity of −40.50 kcal/mol as represented in Fig. 8a and b and Table-10.

3.6.2. *Inter-molecular interaction pattern of 5JLC*

Interaction pattern analysis revealed that Nickel complex displayed the hydrophobic interactions with Tyr127, Lys152, His318 and Leu381 and three weak and one fairly strong electrostatic interaction were found to be generated with Tyr127, Tyr141 and two with Arg386 at a distance of 3.5, 2.8, 3.0 and 3.2 Å respectively, with binding affinity of −10.02 kcal/mol. Meanwhile, the copper complex was observed to generate hydrophobic interactions with Leu381. It established five strong electrostatic interactions with Tyr141, Lys151, Ile473 and two bonds were generated with amino group of Arg386 having distances of 2.8, 3.3, 3.5, 2.6 and 2.9 Å with the biding affinity of −9.51 kcal/mol as represented in Fig. 9a and b and Table-10.

3.6.3. *ADMET profiling*

The physicochemical and pharmacokinetic properties of hit compounds obtained from the docking studies were studied by Swiss ADME. The parameters include Lipinski's rule of five, the solubility of compounds and the potential to cross the blood-brain barrier. As depicted in the Table-11, none of the shortlisted compounds permeated the blood-brain barrier representing a safe profile of the compounds towards the nervous system. The compounds were predicted to have low GI absorption thus making them less oral bio-available referring to the intravenous route of administration. Due to the high molecular weight and presence of a heavy atom, compounds displayed two violations of the Lipinski's rule of five of drug likeness. The *in-silico* toxicity assessments of the shortlisted compounds to estimate their safety profiles were predicted to have LD50 values of 2650 mg/kg for the selected hits. The toxicity classes

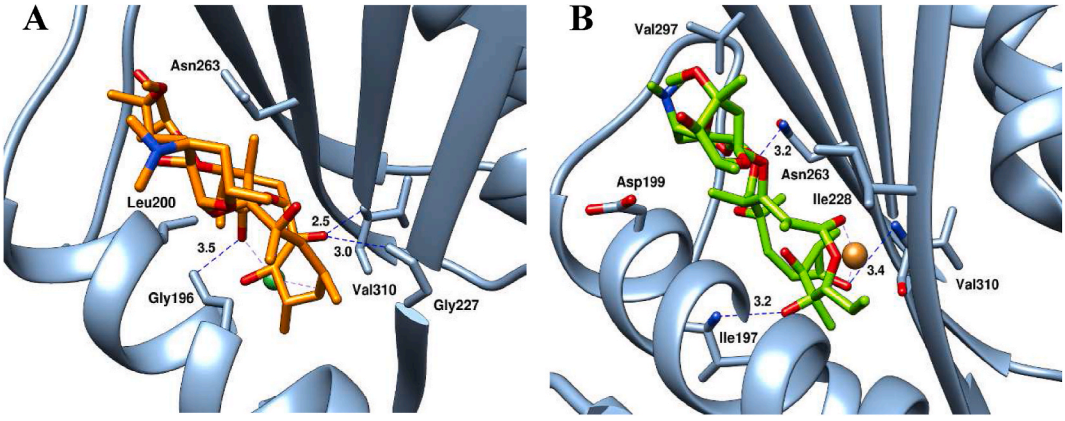

Fig. 8. Docked pose of Ni-complex in orange (a) and Cu-complex in green (b) with 3VOB represented in light blue colour displaying their interactions. (For interpretation of the references to colour in this figure legend, the reader is referred to the Web version of this article.)

Table 10
Interaction Pattern of nickel and copper metal complexes.

Compound	Protein	Binding Energy (kcal/mol)	Hydrogen Bonding	Distance (Å)	Hydrophobic Interactions
Ni-complex	***3VOB***	−41.70	Gly196	3.5	Leu200
			Gly227	3.0	Asn263
			Val310	2.5	
	5JLC	−10.02	Tyr127	3.5	Tyr127
			Tyr141	2.8	Lys152
			Arg386	3.0	His318
			Arg386	3.2	Leu381
Cu-complex	***3VOB***	−40.50	Ile197	3.2	Asn199
			Asn263	3.2	Ile228
			Val310	3.4	Val297
	5JLC	−9.51	Tyr141	2.8	Leu381
			Lys151	3.3	
			Ile473	3.5	
			Arg386	2.6	
			Arg386	2.9	

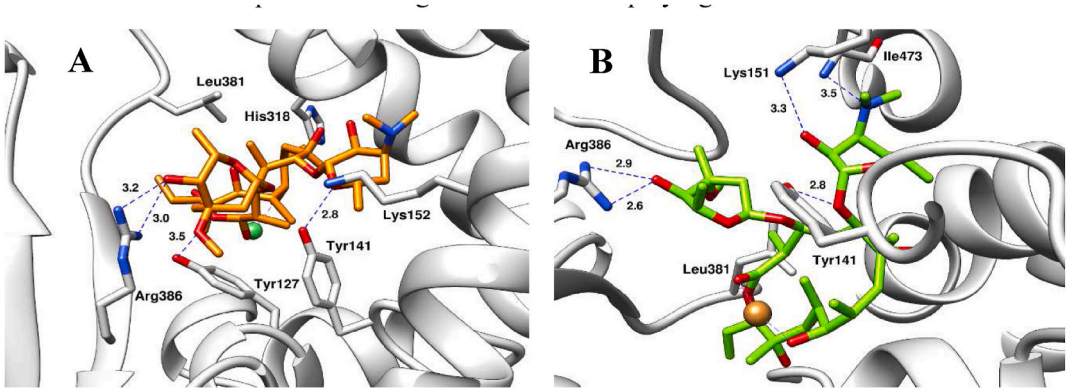

Fig. 9. Docked pose of Ni-complex in orange (a) and Cu-complex in green (b) with 5JLC represented in light grey colour displaying their interactions. (For interpretation of the references to colour in this figure legend, the reader is referred to the Web version of this article.)

Table 11
The Swiss ADME properties of selected compounds.

Compound	Formula	Mol. Weight (g/mol)	Bio-availability score	GI Absorption	BBB permeant	Lipinski's Rule of 5
Ni- complex	$C_{37}H_{64}NNiO_{13}$	789.60	0.11	Low	No	2 violation
Cu-complex	$C_{37}H_{64}CuNO_{13}$	794.45	0.11	Low	No	2 violations

of the compounds predicted belong with class 4 depicting low toxicity and are unlikely to cause significant harm at normal therapeutic doses making them promising candidates for drug development.

4. Conclusion

The synthesis of metal complexes based on erythromycin (Cu, Ni, Co, and Ag) was successfully achieved in a single step, as confirmed by multiple spectroscopic analyses. This study presents a simple method for preparing erythromycin-metal complexes using metal salts in a one-step reaction with free erythromycin from commercially available tablets. The metal salts coordinated, forming stable complexes. These complexes demonstrated antimicrobial activity against various test species, including bacteria and fungi. The antimicrobial susceptibility of specific complexes was examined at varying concentrations, and the effective concentrations needed to inhibit and kill the microorganisms were determined. The synthesized complexes were highly effective against a variety of fungi and bacteria, with compound Ery-Cu having MIC as low as 1.56 mg/mL, Ery-Cu and Ery-Ni with MBCs of 6.25 mg/mL and Ery-Cu having MFC of 6.25 mg/mL. Dose-dependent inhibitory effects were found upon examination of the antimicrobial susceptibility of specific complexes (Cu, Ni, Co and Ag) at varying concentrations of 100, 50, 25 and 12.5 mm/mL. The binding patterns and affinities of the metal complexes with lanosterol 14α-demethylase and Ftsz proteins were clarified by molecular docking simulations, indicating their potential as candidates for structure-based drug design. Complexes of nickel and copper showed significant interactions with important residues of amino acids, suggesting potential use of these compounds in bacterial cell division and fungal infection

therapies. The metal complexes based on erythromycin exhibit promise as antibacterial agents, making them desirable candidates for further pharmacological research. Further research is needed to prove their safety and effectiveness for medicinal uses.

Data availability statement

All data are available in this manuscript.

CRediT authorship contribution statement

Samuel Attah Egu: Supervision, Methodology, Conceptualization. **Lian Ojotule Abah:** Investigation. **Jumai Zainab Hussaini:** Investigation. **Alexander David Onoja:** Resources. **Irfan Ali:** Writing – review & editing. **Atiya Habib:** Software. **Urooj Qureshi:** Software. **Sunday Okpanachi Idih:** Methodology. **Emmanuel Edegbo:** Investigation. **Lawrence Achimugu:** Methodology. **Aminu Omale:** Validation. **Ojochide Charity Michael:** Visualization. **Mohammed Umar Adaji:** Investigation. **Jamila Audu Omale:** Validation, Methodology.

Declaration of competing interest

Authors declare no competing interest.

Acknowledgements

Dr. Samuel Attah Egu is thankful to The World Academy of Sciences, Trieste, Italy, for awarding a prestigious Fellowship for the year 2019–2020 under the TWAS-ICCBS Postdoctoral Fellowship Programme. The authors also acknowledge the financial support of the Pakistan Academy of Science, 3-Constitution Avenue, G-5/2, Islamabad-44000, Pakistan, under Pakistan Academy of Science Project No. 111.

References

[1] S. Prema, Rose A. Leema, Metal complexes of phenyl glycine-O-carboxylic acid: preparation, characterization, electrochemical and biological properties, Orient. J. Chem. 38 (3) (2022) 698.
[2] R.K. Sodhi, S. Paul, Metal complexes in medicine an overview and update from drug design perspective, Cancer Therapy and Oncology International Journal 14 (1) (2019) 25–32.
[3] A.Z. El-Sonbati, M.A. Diab, A.A. El-Bindary, M.I. Abou-Dobara, H.A. Seyam, Molecular docking, DNA binding, thermal studies and antimicrobial activities of Schiff base complexes, J. Mol. Liq. 218 (2016) 434–456.
[4] T. Alorini, I. Daoud, A.N. Al-Hakimi, F. Alminderej, Synthesis, characterization, anticancer activity, and molecular docking study of some metal complexes with a new Schiff base ligand, J. Mol. Struct. 1276 (2023) 134785.
[5] T. Alorini, I. Daoud, A.N. Al-Hakimi, F. Alminderej, A.E. Albadri, An experimental and theoretical investigation of antimicrobial and anticancer properties of some new Schiff base complexes, Res. Chem. Intermed. 49 (4) (2023) 1701–1730.
[6] R.M. Irfan, M.A. Shaheen, M. Saleem, M.N. Tahir, K.S. Munawar, S. Ahmad, M. Mojzych, Synthesis of new cadmium (II) complexes of Schiff bases as alkaline phosphatase inhibitors and their antimicrobial activity, Arab. J. Chem. 14 (10) (2021) 103308.
[7] M. Proetto, W. Liu, A. Hagenbach, U. Abram, R. Gust, Synthesis, characterization and in vitro antitumour activity of a series of novel platinum (II) complexes bearing Schiff base ligands, Eur. J. Med. Chem. 53 (2012) 168–175.
[8] Ö. Şahin, Ü.Ö. Özdemir, N. Seferoğlu, Z.K. Genc, K. Kaya, B. Aydıner, Z. Seferoğlu, New platinum (II) and palladium (II) complexes of coumarin-thiazole Schiff base with a fluorescent chemosensor properties: synthesis, spectroscopic characterization, X-ray structure determination, in vitro anticancer activity on various human carcinoma cell lines and computational studies, J. Photochem. Photobiol. B Biol. 178 (2018) 428–439.
[9] A.N. Al-Hakimi, F. Alminderej, L. Aroua, S.K. Alhag, M.Y. Alfaifi, J.A. Mahyoub, A.S. Alnafisah, Design, synthesis, characterization of zirconium (IV), cadmium (II) and iron (III) complexes derived from Schiff base 2-aminomethylbenzimidazole, 2-hydroxynaphtadehyde and evaluation of their biological activity, Arab. J. Chem. 13 (10) (2020) 7378–7389.
[10] P.P. Netalkar, S.P. Netalkar, S. Budagumpi, V.K. Revankar, Synthesis, crystal structures and characterization of late first row transition metal complexes derived from benzothiazole core: anti-tuberculosis activity and special emphasis on DNA binding and cleavage property, Eur. J. Med. Chem. 79 (2014) 47–56.
[11] F. Firdaus, K. Fatma, M. Azam, S.N. Khan, A.U. Khan, M. Shakir, Template synthesis and physico-chemical characterization of 14-membered tetraimine macrocyclic complexes, $[MLX_2][M=$ Co (II), Ni (II), Cu (II) and Zn (II)]. DNA binding study on $[CoLCl_2]$ complex, Spectrochim. Acta Mol. Biomol. Spectrosc. 72 (3) (2009) 591–596.
[12] G. Indrayanto, G.S. Putra, F. Suhud, Validation of *in-vitro* bioassay methods: application in herbal drug research, Profiles Drug Subst. Excipients Relat. Methodol. 46 (2021) 273–307.
[13] M.L. Magwa, M. Gundidza, N. Gweru, G. Humphrey, Chemical composition and biological activities of essential oil from the leaves of Sesuvium portulacastrum, J. Ethnopharmacol. 103 (1) (2006) 85–89.
[14] B. Pharmacopoeia, in: Monographs: Medicinal and Pharmaceutical Substances. International, 1, 2002, pp. 1889–1892.
[15] L.S. Goodman, A. Gilman, The Pharmacological Basis of Therapeutics, The Macmillan, 1955.
[16] J.E. Reynolds (Ed.), Martindale: the Extra Pharmacopoeia, *thirteenth ed.*, 1993, p. 2400.
[17] V. Vladimir, Andrey Salukhov, Vladimir Nikolaev, Mikhail Ivanov, A.A. Zhurkin, D.A. Chugunov, Marchenko, Multifaceted properties of erdostein and its place in the treatment of respiratory tract diseases, Медицинский совет 16 (18) (2022) 82–89.
[18] M. Ďurišová, Mathematical model of the pharmacokinetic behavior of orally administered erythromycin to healthy adult male volunteers, SOJ Pharmacy and Pharm Sci 3 (1) (2015) 1–5.
[19] Z.Y. He, L.M. Ou, J.Q. Zhang, J. Bai, G.N. Liu, M.H. Li, X.N. Zhong, Effect of 6 months of erythromycin treatment on inflammatory cells in induced sputum and exacerbations in chronic obstructive pulmonary disease, Respiration 80 (6) (2010) 445–452.
[20] A.K. Jindal, K. Pandya, I.D. Khan, Antimicrobial resistance: a public health challenge, Med. J. Armed Forces India 71 (2) (2015) 178–181.
[21] O.A. El-Gammal, A.A. El-Bindary, F.S. Mohamed, G.N. Rezk, M.A. El-Bindary, Synthesis, characterization, design, molecular docking, anti COVID-19 activity, DFT calculations of novel Schiff base with some transition metal complexes, J. Mol. Liq. 346 (2022) 117850.
[22] K.S. Abou-Melha, G.A. Al-Hazmi, I. Althagafi, A. Alharbi, F. Shaaban, N.M. El-Metwaly, M.A. El-Bindary, Synthesis, characterization, DFT calculation, DNA binding and antimicrobial activities of metal complexes of dimedone arylhydrazone, J. Mol. Liq. 334 (2021) 116498.

[23] L. Zhang, L. Guarente, The C6 zinc cluster dictates asymmetric binding by HAP1, EMBO J. 15 (17) (1996) 4676–4681.
[24] Z.H. Chohan, S. Kausar, Synthesis, characterization and biological properties of tridentate NNO, NNS and NNN donor thiazole-derived furanyl, thiophenyl and pyrrolyl Schiff bases and their C< small. letters> o (II), C< small. letters> u (II), N< small. letters> i (II) and Z< small. letters> n (II) metal chelates, Met. Base. Drugs 7 (2000) 17–22.
[25] R.C. Bray, G.N. George, Electron-paramagnetic-resonance studies using pre-steady-state kinetics and substitution with stable isotopes on the mechanism of action of molybdoenzymes, Biochem. Soc. Trans. 13 (1985) 560–567.
[26] G. George, R. Bray, S. Cramer, Extended X-Ray Absorption Fine Structure Studies of Transient Species during Xanthine Oxidase Turnover by Using Rapid Freezing, Portland Press Ltd, 1986.
[27] T.L. Varadinova, P.R. Bontchev, C.K. Nachev, S.A. Shishkov, D. Strachilov, Z. Paskalev, M. Panteva, Mode of action of Zn-complexes on herpes simplex virus type 1 infection *in vitro*, J. Chemother. 5 (1) (1993) 3–9.
[28] S. Rehman, M. Ikram, F. Subhan, M. Sinnokrot, W. Khan, Antibacterial activities of transition metal complexes of mesocyclic amidine 1, 4-diazacycloheptane (DACH), Open Chem. 17 (1) (2019) 936–942.
[29] A.K. Renfrew, Transition metal complexes with bioactive ligands: mechanisms for selective ligand release and applications for drug delivery, Metallomics 6 (8) (2014) 1324–1335.
[30] W.H. Organization, The Evolving Threat of Antimicrobial Resistance: Options for Action, World Health Organization, 2012.
[31] M. Deliorman, F.K. Janahi, P. Sukumar, A. Glia, R. Alnemari, S. Fadl, M.A. Qasaimeh, AFM-compatible microfluidic platform for affinity-based capture and nanomechanical characterization of circulating tumor cells, Microsystems and Nanoengineering 6 (1) (2020) 20.
[32] S.A. Zacchino, S.N. López, G.D. Pezzenati, R.L. Furlán, C.B. Santecchia, L. Muñoz, R.D. Enriz, *In vitro* evaluation of antifungal properties of phenylpropanoids and related compounds acting against dermatophytes, J. Nat. Prod. 62 (10) (1999) 1353–1357.
[33] V.M. Platon, B. Dragoi, L. Marin, Erythromycin formulations—a journey to advanced drug delivery, Pharmaceutics 14 (10) (2022) 2180.
[34] Jyoti Subhash, A. Chaudhary, Synthesis, spectroscopic characterization, in vitro cytotoxic, antimicrobial and antioxidant studies of Co(II) complexes bearing pyridine-based macrocyclic ligands with density function theory (DFT) and molecular docking investigations, Res. Chem. Intermed. 49 (2023) 4729–4758, https://doi.org/10.1007/s11164-023-05096-2.
[35] Jyoti Subhash, A. Phor, et al., Synthesis, structural elucidation, cytotoxic, antimicrobial, antioxidant, density functional theory and molecular docking studies of mononuclear Ru(II) complexes of N_4O_4-bearing macrocyclic ligands, J. Inorg. Organomet. Polym. 34 (2024) 827–847, https://doi.org/10.1007/s10904-023-02862-y.
[36] Jyoti Subhash, M. Gupta, et al., Synthesis, spectral characterisation, in vitro cytotoxicity, antimicrobial, antioxidant, DFT and molecular docking studies of Ru (III) complexes derived from amide-based macrocyclic ligands, Res. Chem. Intermed. 50 (2024) 1081–1111, https://doi.org/10.1007/s11164-023-05124-1.
[37] H.L. Nguyen, P.H. An, N.Q. Thai, H.Q. Linh, M.S. Li, Erythromycin, Cethromycin and Solithromycin display similar binding affinities to the E. coli's ribosome: a molecular simulation study, J. Mol. Graph. Model. 91 (2019) 80–90.
[38] S.H. Rasheed, M. Samanvitha, S.Y. Manjunath, Formulation and in-vitro characterization of erythromycin ocular inserts, International Journal of Research in Pharmaceutical Sciences and Technology 2 (2) (2020) 44–50.
[39] H.L. Nguyen, D.L. Pham, E.P. O'Brien, M.S. Li, Erythromycin leads to differential protein expression through differences in electrostatic and dispersion interactions with nascent proteins, Sci. Rep. 8 (1) (2018) 6460.
[40] E.L. Cyphert, J.D. Wallat, J.K. Pokorski, H.A. Von Recum, Erythromycin modification that improves its acidic stability while optimizing it for local drug delivery, Antibiotics 6 (2) (2017) 11.
[41] J.L. Watts, Performance Standards for Antimicrobial Disk and Dilution Susceptibilty Tests for Bacteria Isolated from Animals: Approved Standard, 1999.
[42] E. Edegbo, D.A. Zakari, P.O. Adejoh, R.O. Raji, C.O. Olaitan, Phytochemical screening and antidermatophytic activity of *Caesalpinia pulcherrima* root extracts on selected dermatophytic isolates, European Journal of Science, Innovation and Technology 2 (1) (2022) 105–112.
[43] J.W. Kennedy, Evaluation of Precision Performance of Clinical Chemistry Devices: Tentative Guideline, National Committee for Clinical Laboratory Standards, 1992.
[44] Molecular Operating Environment (MOE), MOEsaic, PSILO, 2019.
[45] S. Sadeghian, F. Bekhradi, F. Mansouri, R. Razmi, S.G. Mansouri, A. Poustforoosh, Z. Rezaei, Imidazole derivatives as novel and potent antifungal agents: synthesis, biological evaluation, molecular docking study, molecular dynamic simulation and ADME prediction, J. Mol. Struct. 1302 (2024) 137447.
[46] S. Kouser, M. Joythi, A.B. Begum, M.S. Asha, F.H. Al-Ostoot, D.P. Lakshmeesha, S.A. Khanum, Molecular docking, synthesis and antimicrobial evaluation of metal complexes with Schiff base, Results in Chemistry 5 (2023) 100650.
[47] N. Uchikoga, Y. Matsuzaki, M. Ohue, T. Hirokawa, Y. Akiyama, Re-docking scheme for generating near-native protein complexes by assembling residue interaction fingerprints, PLoS One 8 (7) (2013) 69365.
[48] A. Daina, O. Michielin, V. Zoete, SwissADME: a free web tool to evaluate pharmacokinetics, drug-likeness and medicinal chemistry friendliness of small molecules, Sci. Rep. 7 (1) (2017) 42717.
[49] P. Banerjee, A.O. Eckert, A.K. Schrey, R. Preissner, ProTox-II: a webserver for the prediction of toxicity of chemicals, Nucleic acids research 46 (W1) (2018) W257–W263.
[50] A.N.I.N.D.Y.A. Bagchi, P.R.O.S.E.N.J.I.T. Mukherjee, A.N.U.S.R.E.E. Raha, Development and validation of UV spectrophotometric method for estimation of erythromycin in bulk drug and pharmaceutical formulation, Int J Recent Adv. Pharma. Res 5 (2015) 71–76.
[51] H. Kargar, F. Aghaei-Meybodi, R. Behjatmanesh-Ardakani, M.R. Elahifard, V. Torabi, M. Fallah-Mehrjardi, K.S. Munawar, Synthesis, crystal structure, theoretical calculation, spectroscopic and antibacterial activity studies of copper (II) complexes bearing bidentate Schiff base ligands derived from 4-amino-antipyrine: influence of substitutions on antibacterial activity, J. Mol. Struct. 1230 (2021) 129908.
[52] Subhash, A. Chaudhary, Jyoti, M. Kumar, Mamta, R. Solanki, Synthesis, structural elucidation, DFT investigations, biological evaluation and molecular docking studies of tetraamide-based macrocyclic cobalt (II) complexes, J. Iran. Chem. Soc. 20 (9) (2023) 2339–2362.
[53] S. Saravanan, T. Parimelazhagan, *In vitro* antioxidant, antimicrobial and anti-diabetic properties of polyphenols of Passiflora ligularis Juss. fruit pulp, Food Sci. Hum. Wellness 3 (2) (2014) 56–64.
[54] M.M. El-Zahed, M.A. Diab, A.Z. El-Sonbati, M.H. Saad, A.M. Eldesoky, M.A. El-Bindary, Synthesis, spectroscopic characterization studies of chelating complexes and their applications as antimicrobial agents, DNA binding, molecular docking, and electrochemical studies, Appl. Organomet. Chem. 38 (1) (2024) 7290.
[55] A. Sahraei, H. Kargar, M. Hakimi, M.N. Tahir, Synthesis, characterization, crystal structures and biological activities of eight-coordinate zirconium (IV) Schiff base complexes, Transit. Met. Chem. 42 (2017) 483–489.
[56] Subhash, A. Chaudhary, Jyoti, et al., Synthesis, structural elucidation, DFT investigations, biological evaluation and molecular docking studies of tetraamide-based macrocyclic cobalt (II) complexes, J. Iran. Chem. Soc. 20 (2023) 2339–2362, https://doi.org/10.1007/s13738-023-02847-1.
[57] Subhash Mamta, Pinki, A. Chaudhary, In vitro cytotoxicity and antimicrobial evaluation of novel 24–28 membered Schiff base octaazamacrocyclic complexes of manganese(II): synthesis, characterization, DFT and molecular docking studies, J. Mol. Struct. 1275 (2023) 134667, https://doi.org/10.1016/j.molstruc.2022.134667.
[58] Subhash, A. Chaudhary, Mamta, et al., Synthesis, structural characterization, thermal analysis, DFT, biocidal evaluation and molecular docking studies of amide-based Co(II) complexes, Chem. Pap. 77 (2023) 5059–5078, https://doi.org/10.1007/s11696-023-02843-y.
[59] Subhash, A. Chaudhary, Jyoti, et al., Synthesis, spectroscopic characterization, biocidal evaluation molecular docking & DFT investigation of 16-18 membered macrocyclic complexes of cobalt (II), J. Chem. Sci. 134 (2022) 113, https://doi.org/10.1007/s12039-022-02109-2.
[60] H.M. Abd El-Lateef, M.M. Khalaf, A.A. Amer, A.A. Abdelhamid, A. Abdou, Antibacterial, antifungal, anti-inflammatory evaluation, molecular docking, and density functional theory exploration of 2-(1 H-benzimidazol-2-yl) guanidine mixed-ligand complexes: synthesis and characterization, Appl. Organomet. Chem. 38 (1) (2024) 7299.
[61] M.A. El-Bindary, M.G. El-Desouky, A.A. El-Bindary, Metal–organic frameworks encapsulated with an anticancer compound as drug delivery system: synthesis, characterization, antioxidant, anticancer, antibacterial, and molecular docking investigation, Appl. Organomet. Chem. 36 (5) (2022) 6660.

[62] Subhash, A. Chaudhary, Jyoti, M. Kumar, N. Kumar, N.K. Agarwal, Synthesis, spectroscopic characterization, biocidal evaluation molecular docking and DFT investigation of 16-18 membered macrocyclic complexes of cobalt (II), J. Chem. Sci. 134 (4) (2022) 113.
[63] T. Matsui, J. Yamane, N. Mogi, H. Yamaguchi, H. Takemoto, M. Yao, I. Tanaka, Structural reorganization of the bacterial cell-division protein FtsZ from Staphylococcus aureus, Acta Crystallographica Section D: Biological Crystallography 68 (9) (2012) 1175–1188.
[64] R.G. Nelson, A. Rosowsky, Dicyclic and tricyclic diaminopyrimidine derivatives as potent inhibitors of cryptosporidium parvum dihydrofolate reductase: structure-activity and structure-selectivity correlations, Antimicrob. Agents Chemother. 46 (3) (2002) 940.
[65] Subash, M. Kumar, A. Phor, M. Gupta, A. Chaudhary, Design, Synthesis, characterization, in vitro cytotoxic, antimicrobial, antioxidant studies, DFT, Thermal and Molecular docking evaluation of biocompatible Co (II) complexes of N_4O_4-macrocyclic ligands, Comput. Biol. Chem. (2024) 108032.